Temporal dynamics of travelling theta wave activity in infants responding to visual looming

F.R. (Ruud) van der Weel[1] & Audrey L.H. van der Meer[1]

Developmental Neuroscience Laboratory, Department of Psychology, Norwegian University of Science and Technology, NO-7491 Trondheim, Norway

These authors contributed equally to this work

A fundamental property of most animals is the ability to see whether an object is approaching on a direct collision course and, if so, when it will collide. Using high-density electroencephalography in 5- to 11-month-old infants and a looming stimulus approaching under three different accelerations, we investigated how the young human nervous system extracts and processes information for impending collision. Here we show that infants' looming related brain activity is characterized by theta oscillations. Source analyses reveal clear localised activity in the visual cortex. Analysing the temporal dynamics of the source waveform, we provide evidence that the temporal structure of different looming stimuli is sustained during processing in the more mature infant brain, providing infants with increasingly veridical time-to-collision information about looming danger as they grow older and become mobile.

How does the infant brain sense looming danger? Throughout the animal kingdom, the sight of a rapidly approaching object usually signals danger and elicits avoidance reactions[1-3]. An approaching object on a direct collision course projects an expanding image on the retina, providing information that the object is approaching on a collision course and how imminent the collision is. Animal data about the types of neurons that react to such looming stimuli come from studies on the locust[4,5] and the pigeon[6]. Looming stimuli creating travelling waves of neural activity in the visual cortex have been measured in adults[7], and there is ample evidence that the human visual

system is specialized to detect and respond to approaching as opposed to receding motion[8-11]. Infants are also in need of neural structures allowing them to judge impending collisions adequately, especially as their mobility increases during the second half of the first year of life. Behavioural studies on blinking to visual stimuli on collision course[12] and discrimination of changes in heading from optic flow[13] show that prior to the onset of locomotion, infants have problems timing the blink and are less sensitive to optical collisions and flow. Recent developments in non-evasive, high-density electroencephalography (EEG) with sufficiently high temporal resolution allow us to investigate how timing information for impending collision is processed in the infant brain. Research on animal spatial navigation[14,15] highlights the role of theta oscillations in providing a temporal code, suggesting there is spatial information in the precise timing of spikes with respect to the theta rhythm. In infancy, theta activity is strongly related to cognitive and anticipatory attentional processes[16]. Based on these findings, we explore the possibility that event related theta activity in the infant brain can provide the infant with information for impending collision.

To this end, we recorded EEG activity using a Geodesic Sensor Net 200[17] comprising 126 electrodes evenly distributed across the scalp. The vertex electrode (Cz) served as a reference and the EEG was sampled at 500Hz. During the entire experiment corneal reflection (Tobii x50) was used to record gaze of both eyes (50Hz). Using the 'hotspot' visualisation technique (ClearView 2.2.0; Tobii Technology) plotting fixation length over time (see Fig. 1 for a typical example), we excluded trials in which infants did not look for the entire stimulus duration from further analyses. A total of 22 healthy, full-term prelocomotor 5- to 7-, 8- to 9-, and crawling 10- to 11-month-old infants were recruited from newspaper birth announcements. Eighteen (12 boys) provided data for the final sample, six in each age group. Parents gave their informed written consent prior to inclusion in the study according to the Helsinki Declaration. The experimental

setup is shown in Fig. 1 and Supplementary Video 1. (See temporary video preview at: http://www.svt.ntnu.no/psy/NuLab/NatureSuppVid1.html)

Insert Figure 1 about here

A total of 502 trials where the looming stimulus approached the infants on a direct collision course under three different constant accelerations were recorded. Animals have an evolved bias for looming events. Similar to findings obtained from the nucleus rotundus of pigeons[6] and the auditory cortex in monkeys[18], control trials where the virtual object's trajectory did not approach on a direct collision course, but veered off to the left or right or contracted[11], elicited much smaller evoked responses in our infant participants and were therefore not included in the present analyses. Infants were very impressed with our looming stimulus and frequently blinked to protect their eyes. EEG records were inspected for artefacts or poor recordings, and individual channels or localisations within trials were eliminated from the analyses if they occurred, resulting in a rejection rate of 12%. On average, each infant contributed 24 (SD = 8) trials to the experiment.

In order to specifically locate brain activity in response to looming we applied Brain Electrical Source Analysis (BESA 5.1, MEGIS software GmbH[19]). The BESA algorithm estimates the location and the orientation of multiple equivalent dipolar sources by calculating the scalp distribution that would be obtained for a given dipole model (forward solution) and comparing it to the original visual evoked potential (VEP) distribution. Interactive changes in the location and orientation in the dipole sources lead to minimisation of the residual variance between the model and the observed spatio-temporal VEP distribution[20].

Here we used a predefined surrogate dipole model of the visual areas[21] including standard 10-20 sites O1, Oz, and O2. Dipoles at these sites were fitted around peak

looming VEP activity, providing source waveforms (SWF) of the modelled brain regions as a direct measure of their activities on a trial-by-trial basis. Two particular dipoles *VCrL* (visual cortex lateral left) and *VCrR* (visual cortex lateral right) showed consistent symmetrical synchronised activity in response to our looming stimulus. However, brain activity at dipole *VCrL* (see Supplementary Video 2) started earlier ($P < 0.01$) and remained active longer ($P < 0.01$). (See temporary video preview at: http://www.svt.ntnu.no/psy/NuLab/NatureSuppVid2.html)

To analyse the overall effect of looming on oscillatory neuronal synchronisation in dipole *VCrL*, a time-frequency analysis[22] on grand average data across age group and looming speed was performed, showing that evoked event related oscillations in response to the looming stimulus predominantly took place within the theta range (Fig. 2). These findings are consistent with neurophysiological studies in humans showing that theta synchronisation in cortical structures plays an important role in attentional mechanisms providing the necessary conditions for an effective registration and processing of perceptual information[23-25].

Insert Figure 2 about here

By following the same procedure as in [19], a 4-shell ellipsoidal head model was created for every trial, and a predefined model of the visual cortex was inserted as dipoles into the head model. This model was then applied to the raw data transforming the EEG scalp signal to separate brain space signals (see Supplementary Fig. 1) resulting in a new EEG voltage sequence over time. The results of this analysis for source waveform activity at dipole *VCrL* (Fig. 3a, dipole shown in head model in blue) are shown for the three infant age groups (Fig. 3b-d). Overall shape of the source waveforms was similar at the different ages. However, source waveform duration ranged from relatively short durations of about 50 ms in the 10- to 11-month-olds to

twice as long durations in the 5- to 7-month-olds, revealing a significant developmental trend in processing time ($F(2,15) = 7.07$, $P < 0.01$).

Insert Figure 3 about here

Source waveform activity *per se* did not discriminate well between looms. Therefore, we performed an extrinsic tau-coupling analysis[26-28] on the *VCrL* SWF. For each trial, the desynchronization phase of the SWF and its rate of change were plotted against time (Fig. 4a), as well as the corresponding visual angle of the looming stimulus and its rate of change (Fig. 4b). The peak velocity of each SWF was identified and demarcated at 10%, or as close to 10% as possible, of this value. The tau of SWF activity during desynchronization (i.e., the tau values between the beginning and end of desynchronization, τ_{SWF}) and the corresponding tau of the loom (τ_{loom}) were calculated using the general equation: $\tau(x) = x/\dot{x}$ (Fig. 4c) and plotted against each other (Fig. 4d). Finally, a recursive linear regression analysis was run on the plot to determine the strength of the coupling between τ_{SWF} and τ_{loom} (measured by the r^2 value of the regression) and to estimate the value of the constant K in the tau-coupling equation $\tau_{SWF} = K\tau_{loom}$ (measured by the slope of the regression), by removing the leftmost points in the plot one by one until the r^2 of the regression exceeded the criterion level which was set at 0.95, thus ensuring that 95% of the variance in the data was explained by a linear model. The percentage of the SWF during which it is tau-coupled to the loom was calculated by dividing the remaining points in the plot by the total number in the SWF. For the data presented in Fig. 4d the percentage tau-coupling was 79.4%, the r^2 of the tau-coupling was 0.959, and the regression slope was 1.516. High percentages of extrinsic tau-coupling and high r^2 values allow for the regression slope to be a good estimator of the coupling constant K.

Insert Figure 4 about here

Averaged time-normalised tau-couplings are shown for the three looms for each of the three infant age groups separately (Fig. 3e-g). Values of K were significantly > 1 for all age groups and all looms (slow: $t(17) = 3.03$, $P < 0.01$; medium: $t(17) = 3.95$, $P < 0.005$; fast: $t(17) = 6.64$, $P < 0.001$), reflecting well the accelerating nature of our looming stimulus which hit the infants in the face at high velocity. When $K > 1$, as in our case, desynchronization of the SWF ends with progressively increasing acceleration. In comparison, K values between $0 < K < 1$ would indicate that SWF desynchronization ended while decelerating (see [26] for mathematical proof). A repeated measures ANOVA revealed a significant loom x group interaction ($F(4,30) = 3.225$, $P < 0.03$), indicating that the 10- to 11-month-olds differentiated well between the three looms with increasing values of K for faster looms, while the younger infants did not. Especially the 5- to 7-month-olds, judging by their K values all lying around 1.3, appeared to process all looms as if they were fast looms (Fig. 3g). These findings suggest well-established neural networks for registering impending collision in 10- to 11-month-olds, but not yet in 5- to 7-month-olds. The 8- to 9-month-old infants displayed an in-between developmental stage. This could be interpreted as a sign that appropriate neural networks are in the process of being established and that the age of 8-9 months would be an important age for doing so. Coincidentally, this is also the average age at which infants start crawling. This makes sense from a perspective where brain and behavioural development go hand-in-hand[29]. Namely, as infants gain better control of self-produced locomotion, their perceptual abilities for sensing looming danger improve.

We propose that as a function of perceptuo-motor development the temporal structure of looming information is increasingly well differentiated in the neural circuitry of the infant brain, providing infants with important time-to-collision information. By analysing the tau of theta oscillations in the visual cortex in response to the looms we were able to reveal a temporal structure of theta activity that is consistent with that present in the looming information. Tau of a neural current is biologically

viable neural information because it would flow through neural networks with its value being unaffected by changes in the impedances of the synapses. In contrast, the amplitude of neural current would be distorted by such factors, and so is not as robust information. Our results suggest that when looming-related electric energy is travelling through the infant brain, its temporal structure provides the appropriate brain parts with veridical sensory looming information. Judging from the spatial location and temporal progression of our *VCrL* dipole, a likely area for processing this type of information would be where brain signals are progressing from visual cortical area V1 to V3 and V5/MT+, the (extra)striate areas (cf. [30]).

1. Schiff, W. Perception of impending collision: A study of visually directed avoidant behavior. *Psychol. Monogr.* **79,** 1-26 (1965).

2. Schiff, W., Caviness, J. A. & Gibson, J. J. Persistent fear response in rhesus monkeys to the optical stimulus of "looming". *Science* **136,** 982-983 (1962).

3. Martinoya, C. J. & Delius, D. Perception of rotating spiral patterns by pigeons. *Biol. Cybern.* **63,** 127-134 (1990).

4. Hatsopoulos, N., Gabbiani, F. & Laurent, G. Elementary computation of object approach by a wide-field visual neuron. *Science* **270,** 1000-1003 (1995).

5. Rind, F. C. & Simmons, P. J. Signaling of object approach by the DCMD neuron of the locust. *J. Neurophysiol.* **77,** 1029-1033 (1997).

6. Sun, H. & Frost, B. J. Computation of different optical variables of looming objects in pigeon nucleus rotundus neurons. *Nature Neurosci.* **1,** 296-303 (1998).

7. Dougherty, R. F. *et al.* Visual field representations and locations of visual areas V1/2/3 in human visual cortex. *J. Vision* **3,** 586-598 (2003).

8. Morrone M. C. *et al.* A cortical area that responds specifically to optic flow, revealed by fMRI. *Nature Neurosci.* **3,** 1322-1328 (2000).

9. Ptito, M., Kupers, R., Faubert, J.& Gjedde, A. Cortical representation of inward and outward radial motion in man. *NeuroImage* **14,** 1409-1415 (2001).

10. Shirai, N. & Yamaguchi, M. K. Asymmetry in the perception of motion-in-depth. *Vis. Res.* **44,** 1003-1011 (2004).

11. Holliday, I. E. & Meese, T. S. Neuromagnetic evoked responses to complex motions are greatest for expansion. *Int. J. Psychophysiol.* **55,** 145-157 (2005).

12. Kayed, N. S. & Van der Meer, A. L. H. Infants' timing strategies to optical collisions: A longitudinal study. *Infant Behav. Dev.* **30,** 50-59 (2007).

13. Gilmore, R. O., Baker, T. J. & Grobman, K. H. Stability in young infants' discrimination of optic flow. *Dev. Psychol.* **40,** 259-270 (2004).

14. O'Keefe, J. & Recce, M. L. Phase relationship between hippocampal place units and the EEG theta rhythm. *Hippocampus* **3,** 317-330 (1993).

15. Mehta, M. R., Lee, A. K. & Wilson, M. A. Role of experience and oscillations in transforming a rate code into a temporal code. *Nature* **417,** 741-746 (2002).

16. Orekhova, E. V., Stroganova, T. A. & Posikera, I. N. Theta synchronization during sustained anticipatory attention in infants over the second half of the first year of life. *Int. J. Psychophysiol.* **32,** 151-172 (1999).

17. Tucker, D. M. Spatial sampling of head electric fields: The Geodesic sensor net. *Electroencephalogr. Clin. Neurophysiol.* **87,** 154-163 (1993).

18. Maier, J. X. & Ghazanfar, A. A. Looming biases in monkey auditory cortex. *J. Neurosci.* **27,** 4093-4100 (2007).

19. Hoechstetter, K. *et al.* BESA source coherence: A new method to study cortical oscillatory coupling. *Brain Topography* **16,** 233-238 (2004).

20. Scherg, M. in *Auditory Evoked Magnetic Fields and Electric Potentials: Advances in Audiology* (eds Grandori, F., Hoke, M. & Romani, G. L.) 40-69 (Karger, 1990).

21. Di Russo, F., Martinez, A., Sereno, M. I., Pitzalis, S. & Hillyard, S. A. Cortical sources of the early components of the visual evoked potential. *Hum. Brain Mapp.* **15,** 95-111 (2001).

22. Tallon-Baudry, C., Bertrand, O., Perronnet, F. & Pernier, J. Induced gamma-band activity during the delay of a visual short-term memory task in humans. *J. Neuroscience* **18,** 4244-4254 (1998).

23. Kahana, M. J., Seelig, D. & Madsen, J. M. Theta returns. *Curr. Opin. Neurobiol.* **11,** 739-744 (2001).

24. Vinogradova, O. S. Expression, control, and probable functional significance of the neuronal theta-rhythm. *Prog. Neurobiol.* **45,** 523-583 (1995).

25. Pfurtscheller, G. & Lopes da Silva, F. H. Event-related EEG/MEG synchronization and desynchronization: Basic principles. *Clin. Neurophysiol.* **110,** 1842-1857 (1999).

26. Lee, D. N. Guiding movement by coupling taus. *Ecol. Psychol.* **10,** 221-250 (1998).

27. Lee, D. N., Georgopoulos, A. P., Clark, M. J. O., Craig, C. M. & Port, N. L. Guiding contact by coupling the taus of gaps. *Exp. Brain Res.* **139,** 151-159 (2001).

28. Kayed, N. S. & Van der Meer, A. L. H. A longitudinal study of prospective control in catching by full-term and preterm infants. *Exp. Brain Res.*, in press (available at http://www.springerlink.com/content/78q901h65r89l1q4/?p=dcf7494dfe864614b4ab1e29e61f8f63&pi=10)

29. Johnson, M. H. Functional brain development in infants: Elements of an interactive specialization framework. *Child Dev.* **71,** 75-81 (2000).

30. Di Russo F. *et al.* Identification of the neural sources of the pattern-reversal VEP. *NeuroImage* **24**, 874-886 (2005).

Supplementary Information is linked to the online version of the paper at www.nature.com/nature.

Acknowledgements We are grateful to all the infants and their parents for taking part in this study. We also thank D. N. Lee for discussion, G. –J. Pepping for providing us with the tau analysis software, S. Houweling and J. F. Léger for programming the looming stimuli, and M. Holth for testing assistance.

Author Contributions Both authors contributed equally to this work.

Author Information Correspondence and requests for materials should be addressed to F.R.W. (ruudw@svt.ntnu.no).

Figure 1. The experimental setup and diagram of stimulus configuration (**a**) and procedure (**b**). Each infant was shown a semi-randomised sequence of an image of a circular disk on a collision course. As the virtual object approaches the eye, its image size on the screen grows. The looming stimulus simulated an object coming from far away (subtending 5° at the eye, θ) approaching for a duration of 2, 3, and 4s under three different constant accelerations (21.1, 9.4, and 5.3 m/s^2, respectively), and finally 'hitting' the infants in the face (θ = 131°). Movement stopped when the image filled the entire screen.

Figure 2. Temporal-spectral evolution of percentage amplitude change at source *VCrL*. Time-frequency display of grand average data (across age groups and looms) where the amplitude for each time instant is normalised to the mean amplitude of the baseline epoch for that frequency. To this end, individual looming trials were aligned by peak amplitude and analysed with an epoch length of -300:300 ms and a baseline of -300:-200 ms. Spectral change over time at dipole *VCrL* is indicated by the red cloud in the background indicating an overall 63% increase in activity between 0.1–7.5 Hz. The outlined areas in red, blue, and black indicate where a significant increase in brain activity was found for the three age groups separately. These were between 0.1–8 Hz (delta/theta/alpha range) for the 5- to 7-month-olds ($P < 0.001$), between 4–7 Hz (theta range) for the 8- to 9-month-olds ($P < 0.001$), and between 2-6 Hz (delta/theta range) for the 10- to 11-month-olds ($P < 0.005$).

Figure 3. (**a**) Accelerating looming stimulus approaching the infants' eyes resulting in increased theta activity in the visual cortex. A 4-shell ellipsoidal head model was created for every trial and used as a source montage to transform the recorded EEG data from electrode level into brain source space. The results of this analysis for dipole *VCrL* (depicted in head model in blue) are shown for the three infant age groups (**b-d**). Each graph shows average, peak-

aligned source waveform activity at dipole *VCrL* (including standard error bars) for the three looms. Overall shape of the source waveforms was similar at the different ages, but their duration was about twice as long in the 5- to 7-month-olds as compared to the 10- to 11-month-olds. Source waveform activity did not discriminate well between looms. Therefore, the source waveform was tau-coupled[26,27] onto the loom to study the temporal dynamics of neural activity (see Fig. 4). (**e-g**) Average tau-coupling plots, τ_{SWF} vs τ_{loom} (including standard error bars), for each age group for the three looms, showing that crawling 10- to 11-month-olds differentiated well between looms, whereas younger prelocomotor infants did not.

Figure 4. Tau-coupling analysis. Two variables, X and Y, are tau-coupled if $\tau_{(X)} = K\tau_{(Y)}$, where *K* is a coupling constant. (**a**) Showing how SWF activity, X, and its rate of change, $\dot{X}$, changed continuously during a typical infant's brain response to a fast loom (**b**) Showing how the visual angle of the looming stimulus, *Y,* and its rate of change, $\dot{Y}$, increased continuously during the loom's progression. The tau of SWF activity ($\tau_{(X)}$, or $X/\dot{X}$) during desynchronization (area between vertical lines) is plotted against time in (**c**) together with the corresponding tau for the loom ($\tau_{(Y)}$, or $Y/\dot{Y}$). (**d**) Plotting $\tau_{(X)}$ against $\tau_{(Y)}$ in order to find the percentage tau-coupling by means of a recursive linear regression. To ensure that 95% of the variance in the data was explained by a linear model, only regression strengths of $r^2 > 0.95$ were accepted, meaning that the first seven data points from the original data set were omitted. The remaining points in the plot were divided by the total number of points in the desynchronization, providing an estimate of how much of the SWF was tau-coupled to the loom. Here, percentage tau-coupling was 79.4%, r^2 of the coupling 0.959, and the regression slope 1.516.

Supplementary Online Information

Supplementary Figure 1

(**a**) Raw EEG data of a single 2s (fast) looming trial displayed using standard 10-20 sites. Note increased activity at sites O1, Oz and O2 as a direct response to the loom, with vertical yellow line marking peak activity. The inserted 3D mapping window visualizes a build-up and decline over time of EEG voltage in the visual cortex (0 ms = peak activity at vertical yellow line) (see Supplementary Video 3). (See temporary video preview at: http://www.svt.ntnu.no/psy/NuLab/NatureSuppVid3.html).

(**b**) Source analysis of the same trial, using a predefined surrogate dipole model of the visual areas[21], including O1, Oz, and O2. Dipoles at these sites were fitted -200:200 ms around peak VEP activity as indicated by yellow line in (**a**), providing source waveforms (SWF) of the modelled brain regions as a direct measure of their activities on a trial-by-trial basis (centre lower panel). Two dipoles, *VCrL* (blue curve) and *VCrR* (red curve), showed consistent symmetrical synchronised activity in response to our looming stimulus. Top right panel shows the relative contribution (position and direction) of each dipole to the model. Bottom right panel shows a Multiple-Source Beam Former image of evoked brain responses to the looming stimulus, revealing involvement of primary visual areas in the occipital cortex and of the right-hemispheric MT+ area (see Supplementary Video 2).

Supplementary Video 1: The looming stimulus

This movie shows an 8-month-old infant ready for testing and a diagram of our experimental setup (see also Fig. 1). The infant is watching the looming stimuli approaching under three different accelerations. The blue dot moving in the middle of the looming circle represents the infant's gaze of both eyes collected by the Tobii eye-tracker and was used to confirm that the infant was attending the looming stimuli (Quicktime; MPEG4; 14 226KB). For temporary video preview see: (http://www.svt.ntnu.no/psy/NuLab/NatureSuppVid1.html)

Supplementary Video 2: *VCrL* dipole activity

This movie shows *VCrL* dipole source waveform activity in the O1 region of an 8-month-old infant in response to a medium loom (9.4 m/s^2). Activity is shown in slow motion (see running time in ms) for clarity. (Quicktime; MPEG4; 16 706KB). For temporary video preview see: (http://www.svt.ntnu.no/psy/NuLab/NatureSuppVid2.html)

Supplementary Video 3: VEP surface activity

This movie shows in real time VEP surface activity in the O1, Oz, O2 region (in blue) in response to a fast loom (21.1 m/s^2) in an 8-month-old infant. The same trial is also repeated in slow motion for clarity (Quicktime; MPEG4; 5 003KB). For temporary video preview see: (http://www.svt.ntnu.no/psy/NuLab/NatureSuppVid3.html)

Supplementary Cover Proposal 1: The looming stimulus (large circle with four brightly colored inner circles) and resulting brain activity in a spatio-temporal cortical map superimposed on photographs of infant participants.

Supplementary Cover Proposal 2: The looming stimulus (large circle with four brightly colored inner circles) and resulting brain activity in a spatio-temporal cortical map superimposed on the photograph of a participating infant.

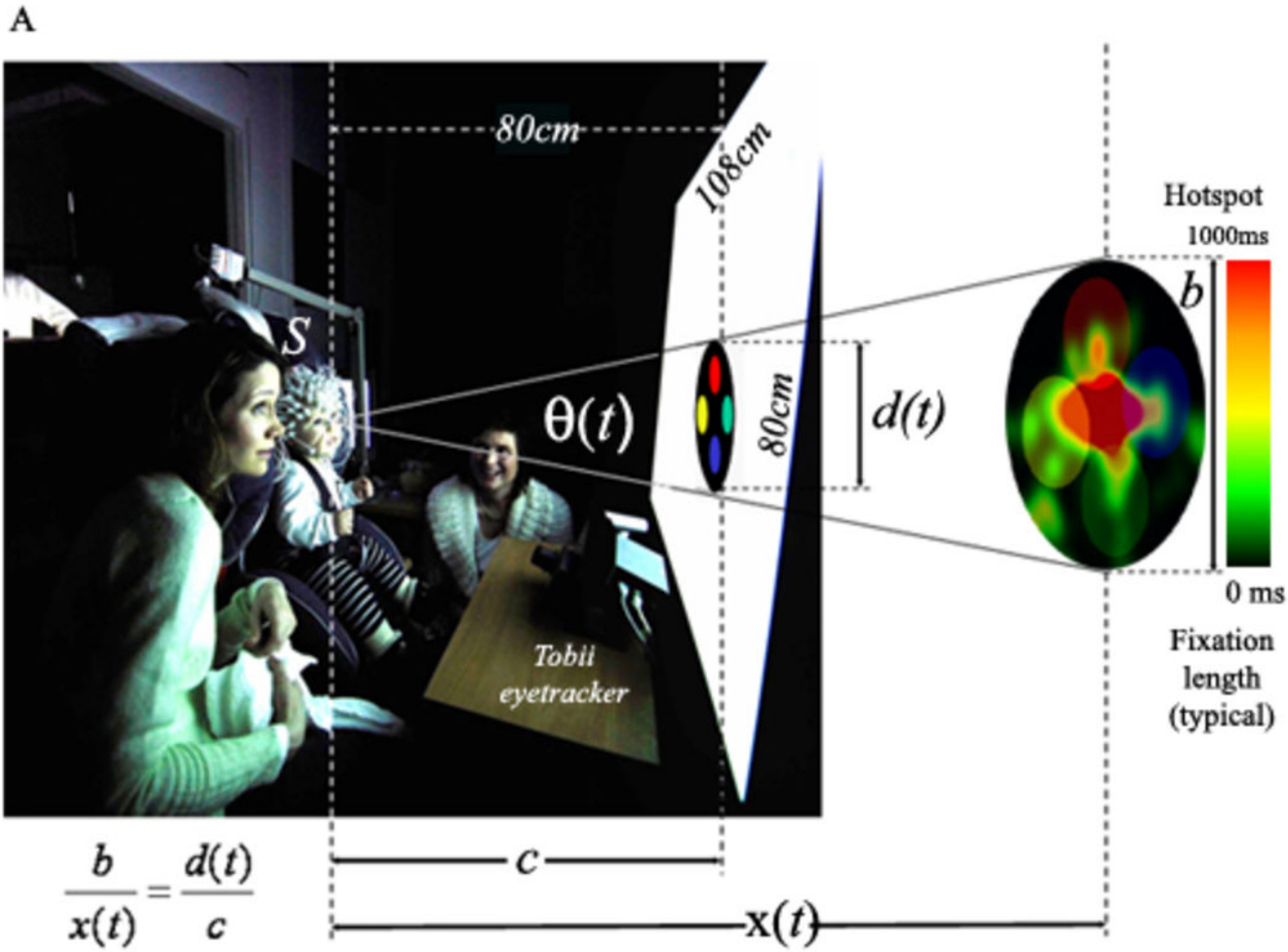
A
80cm
108cm
S
θ(t)
80cm
d(t)
b
Hotspot
1000ms
0 ms
Fixation
length
(typical)
Tobii
eyetracker
b / x(t) = d(t) / c
c
x(t)

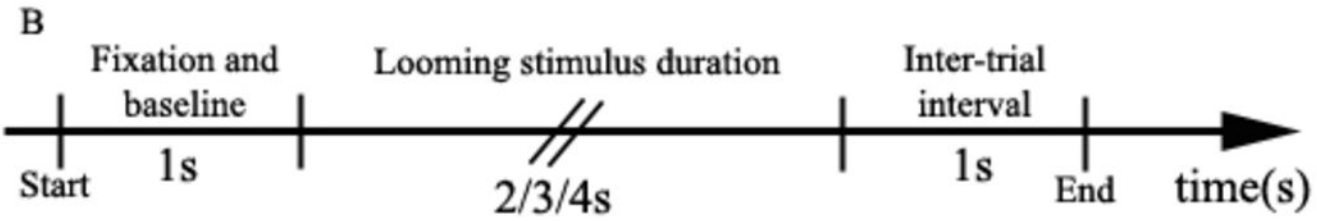
B
Fixation and
baseline
1s
Looming stimulus duration
2/3/4s
Inter-trial
interval
1s
Start
End
time(s)

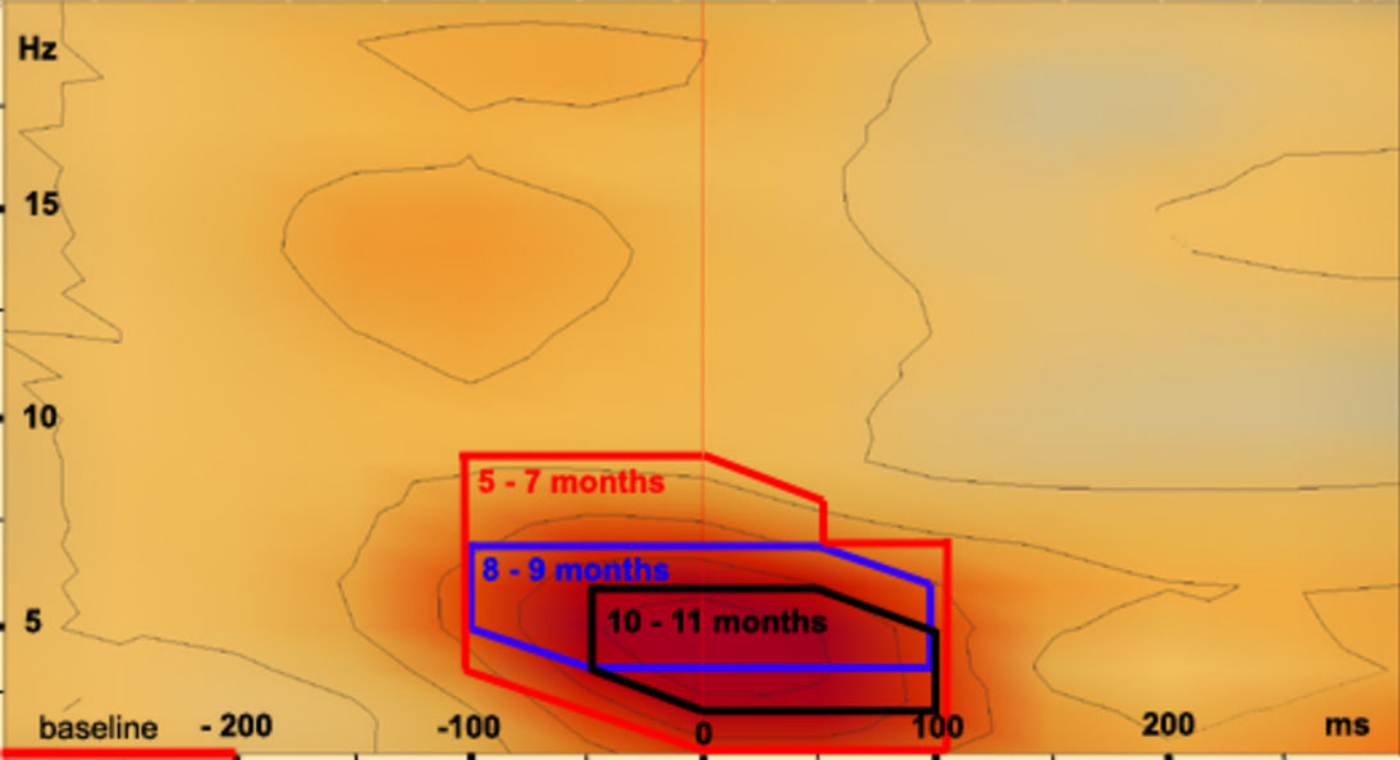
Hz
15
10
5
5 - 7 months
8 - 9 months
10 - 11 months
baseline
- 200
-100
0
100
200
ms

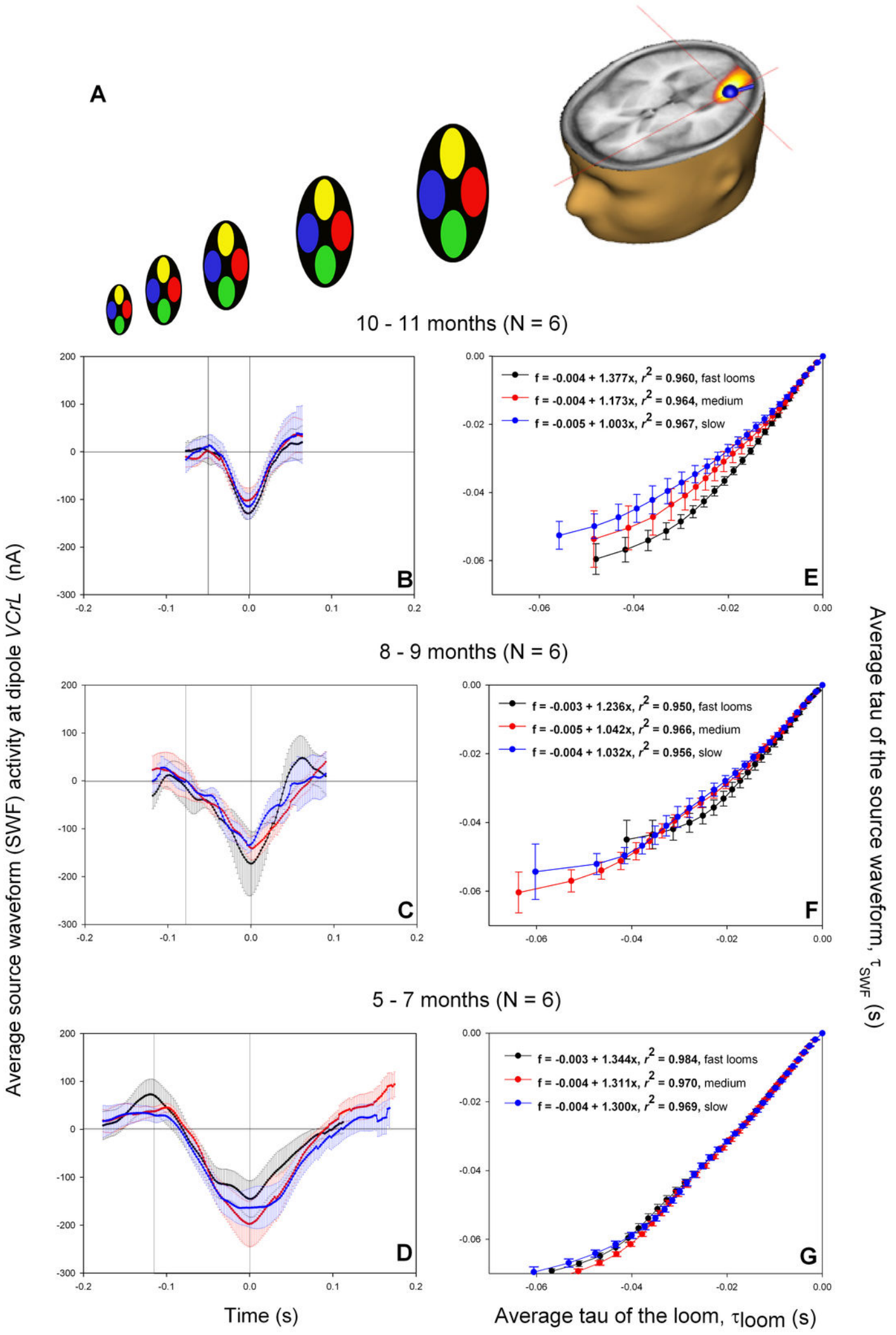
A
10 - 11 months (N = 6)
8 - 9 months (N = 6)
5 - 7 months (N = 6)
B
C
D
E
F
G
f = -0.004 + 1.377x, r2 = 0.960, fast looms
f = -0.004 + 1.173x, r2 = 0.964, medium
f = -0.005 + 1.003x, r2 = 0.967, slow
f = -0.003 + 1.236x, r2 = 0.950, fast looms
f = -0.005 + 1.042x, r2 = 0.966, medium
f = -0.004 + 1.032x, r2 = 0.956, slow
f = -0.003 + 1.344x, r2 = 0.984, fast looms
f = -0.004 + 1.311x, r2 = 0.970, medium
f = -0.004 + 1.300x, r2 = 0.969, slow
Average source waveform (SWF) activity at dipole VCrL (nA)
Time (s)
Average tau of the loom, τloom (s)
Average tau of the source waveform, τSWF (s)

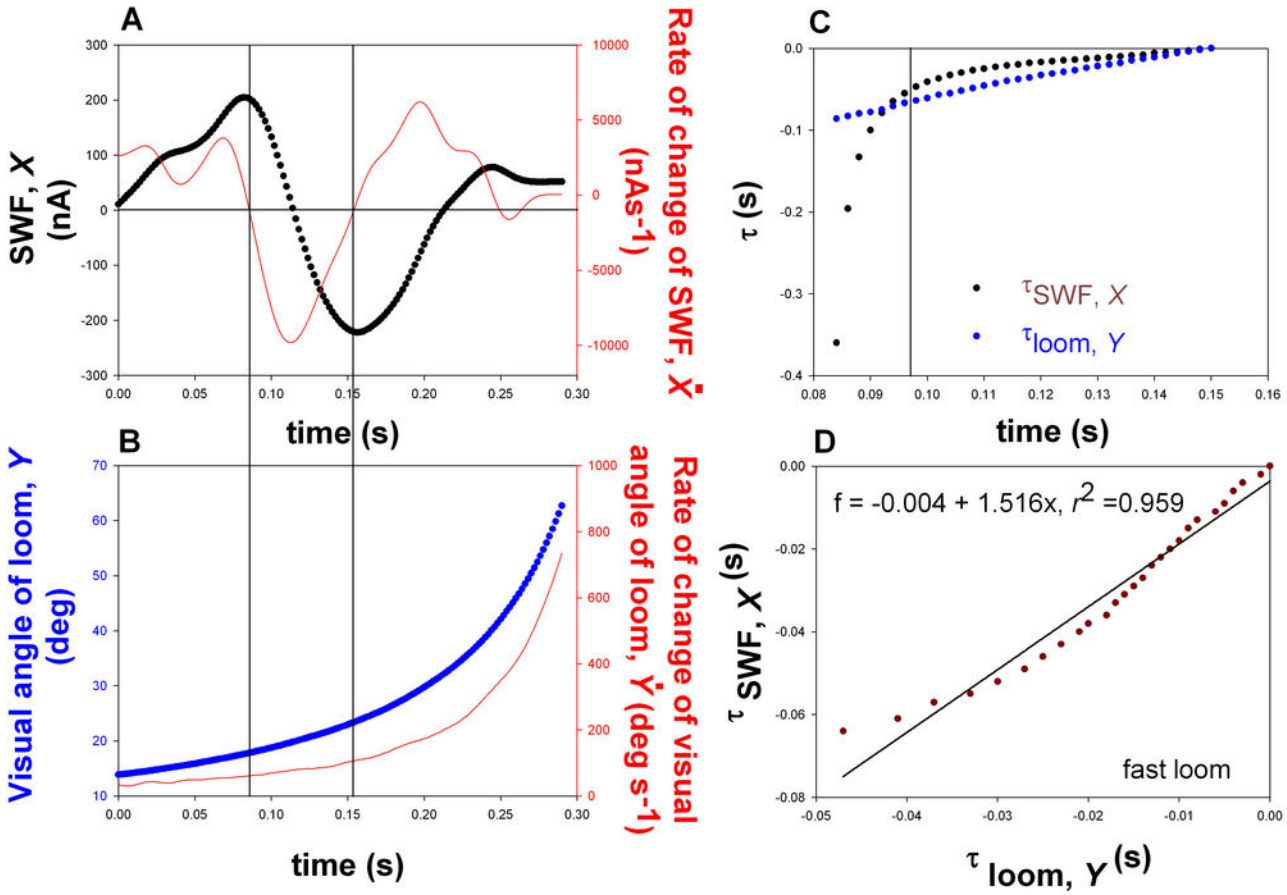
A
SWF, X (nA)
Rate of change of SWF, Ẋ (nAs-1)
time (s)
B
Visual angle of loom, Y (deg)
Rate of change of visual angle of loom, Ẏ (deg s-1)
time (s)
C
τ (s)
τSWF, X
τloom, Y
time (s)
D
τ SWF, X (s)
f = -0.004 + 1.516x, r2 =0.959
fast loom
τ loom, Y (s)